International Journal of Remote Sensing

Publication details, including instructions for authors and subscription information:
http://www.tandfonline.com/loi/tres20

Vertical scaling of temperature, wind and humidity fluctuations: dropsondes from 13 km to the surface of the Pacific Ocean

Susan J. Hovde [a b], Adrian Francis Tuck [c d e], Shaun Lovejoy [f] & Daniel Schertzer [d e]

[a] NOAA Earth System Research Laboratory, Chemical Sciences Division, Boulder, CO, 80305, USA

[b] Cooperative Institute for Research in Environmental Science, University of Colorado, Boulder, CO, 80309, USA

[c] Department of Physics, Imperial College London, London, SW7 2AZ, UK

[d] Laboratoire Eau Environnement Systèmes Urbains, École Nationale des Ponts-Paris Tech, Université de Paris-Est, 77455 Cedex 02, France

[e] Department of Physics, McGill University, Montréal, QC, Canada, H3A 2T8

[f] Centre GEOTOP UQAM-McGill Université du Québec à Montréal, Montréal, QC, Canada, H3C 3P8

Available online: 22 Aug 2011

To cite this article: Susan J. Hovde, Adrian Francis Tuck, Shaun Lovejoy & Daniel Schertzer (2011): Vertical scaling of temperature, wind and humidity fluctuations: dropsondes from 13 km to the surface of the Pacific Ocean, International Journal of Remote Sensing, DOI:10.1080/01431161.2011.602652

To link to this article: http://dx.doi.org/10.1080/01431161.2011.602652

International Journal of Remote Sensing
iFirst, 2011, 1–28

Vertical scaling of temperature, wind and humidity fluctuations: dropsondes from 13 km to the surface of the Pacific Ocean

SUSAN J. HOVDE†‡, ADRIAN FRANCIS TUCK*§¶, SHAUN LOVEJOY†† and DANIEL SCHERTZER¶

†NOAA Earth System Research Laboratory, Chemical Sciences Division, Boulder, CO 80305, USA
‡Cooperative Institute for Research in Environmental Science, University of Colorado, Boulder, CO 80309, USA
§Department of Physics, Imperial College London, London SW7 2AZ, UK
¶Laboratoire Eau Environnement Systèmes Urbains, École Nationale des Ponts-Paris Tech, Université de Paris-Est, 77455 Cedex 02, France
¶Department of Physics, McGill University, Montréal, QC, Canada H3A 2T8
††Centre GEOTOP UQAM-McGill Université du Québec à Montréal, Montréal, QC, Canada H3C 3P8

(*Received 8 December 2010; in final form 27 April 2011*)

Observational data were taken in the 'vertical' structure at 2 Hz from research dropsondes for temperature, wind speed and relative humidity during the ~800 s it takes to reach the surface from the ~13 km altitude of the National Oceanic and Atmospheric Administration (NOAA) Gulfstream 4SP aircraft. The observations were made mainly through the depth of the troposphere above the eastern Pacific Ocean from 15° N to 43° N (dropsondes) and 60° N (aircraft) in 2004. Grand averages of some key figures and of probability distribution functions (PDFs) were formed by compounding the data from the Winter Storms Projects 2004, 2005 and 2006, comprising 246, 324 and 315 (some dropped up to 60° N) useable sondes, respectively. This sizeable data set was used to representatively characterize the statistical fluctuations in the 'vertical' structure from 13 km to the surface. The fluctuations are resolved at 5–10 m altitude, so covering up to 3 orders of magnitude of typical tropospheric weighting functions for passive remote sounders. Average 'vertical' statistical, multifractal, scaling exponents H, C_1 and α of temperature, wind speed and humidity fluctuations observed at high resolution were computed and are available as potential generators of representative, scale-invariant summaries of the vertical structure of the marine troposphere, for use in design and retrieval of remotely sounded observations.

1. Introduction

Detailed high-resolution information from research quality observations of the vertical fluctuations in the structure of tropospheric variables over the large oceanic area between 15° N and 60° N, bounded longitudinally by the dateline and the west coast of North America, has value for remote sounding retrievals in the nadir, given the paucity

*Corresponding author. Email: dr.adrian.tuck@sciencespectrum.co.uk

International Journal of Remote Sensing
ISSN 0143-1161 print/ISSN 1366-5901 online © 2011 Taylor & Francis
http://www.tandf.co.uk/journals
DOI: 10.1080/01431161.2011.602652

of such information. The value from the Global Positioning System (GPS) dropsondes is further enhanced by considering similar information in the horizontal from the parent aircraft itself, providing additional information in the limb scanning context. Its utility also includes improving the performance of synoptic weather forecasting and climate models (MacDonald 2005) and investigating the tropospheric chemical composition (Cooper *et al*. 2005). Basic theoretical interpretations of observed atmospheric structure above the ocean provide a means of providing compact descriptions, via the scaling exponents calculated by the application of generalized scale invariance, of the statistics of the fluctuations obtained at high resolution. The fluctuations concern the roles of isotropy, anisotropy and invariance and their direct potential importance for remote sounding retrievals, as contrasted to the flux and cascade interpretations drawn from the data, whose conceptual importance has been described elsewhere (Lovejoy *et al*. 2009a).

We use tropospheric observations made from GPS dropsondes (Hock and Franklin 1999), telemetered back to the parent National Oceanic and Atmospheric Administration (NOAA) Gulfstream 4SP aircraft during the Winter Storms 2004 Project over the eastern Pacific Ocean in the first 3 months of the year, between 10° N and 60° N, for our primary analysis. Most of the flights described here had both take-off and landing at Honolulu (21° N, 158° W), but the consecutive flights on 05, 06 and 08 March 2004 were from Honolulu, Anchorage (61° N, 150° W) and Long Beach (34° N, 118° W). Additionally, we use similar observations from 2005 and 2006 to compile probability distribution functions (PDFs) that are representative of the vertical structure of the full troposphere above the eastern extratropical Pacific Ocean within this large marine area. While the primary analysis has been carried out for the case in 2004, when sondes were dropped along purposely designed – largely great circle – flight segments, the data from 2005 and 2006 were included with the 2004 data to form enhanced grand averages for appropriate variables connected with the vertical structure of temperature, winds and humidity. There were 324 useable sondes out of a total of 363 dropped in 2005 in the area bounded by 21° N–45° N and 132° W–182° W and 315 useable out of 352 dropped in 2006 in the area bounded by 21° N–60° N and 128° W–172° W. During the 2006 mission, sondes were dropped between 46° N and 60° N for the first time, when the aircraft was based in Anchorage for a significant fraction of the time.

The observations from the dropsondes are given a horizontal context and were made possible by the significant difference between the scaling structure of the G4 aircraft data in the 'vertical' and in the 'horizontal'. 'Vertical' ascents and descents from the National Aeronautical and Space Administration (NASA) WB57F research aircraft at about 10° N, 84° W during the first 2 months of 2004 allow some extension to the tropics. It is not currently possible for our purposes to obtain atmospheric observations with adequate spatial and temporal resolution that are truly vertical and horizontal, because the effects of atmospheric variation upon the motion of the platform mix the two coordinates, whether aircraft or balloons are used. Nevertheless, there is internal consistency between the aircraft ascents and descents and the dropsonde data; their similarity to each other and their dissimilarity to the 'horizontal' aircraft data are important supporting facts in the validity of the scaling exponents as compact summaries of the statistics of the fluctuations observed.

The theory of generalized scale invariance (Schertzer and Lovejoy 1985, 1987, 1991) has been applied successfully to a large volume of airborne atmospheric data, acquired from high altitude aircraft, largely in the lower stratosphere (Tuck and Hovde 1999,

Tuck *et al*. 2002, 2003a, b, 2004, 2005, Lovejoy *et al*. 2004). Generalized scale invariance has been reviewed recently, in a solid earth geophysical context, by Lovejoy and Schertzer (2007). The effect of the G4 aircraft motion in 'horizontal' flight in the stratosphere under autopilot control operating isobarically was examined by Lovejoy *et al*. (2009b), who showed that the scale-by-scale conservation scaling exponents $H_a(s)$ and $H_a(T)$, could be anomalous due to long-range correlations between the aircraft motion and the wind field (the subscript a denotes observations made from an aircraft, s the wind speed and T the temperature; for fluctuations Δf in a quantity f, over a distance Δx we have $< \Delta f > \approx \Delta x^H$). Note that the conservation or Hurst exponent H is defined by equations given, most recently, in Tuck (2010) and refers to the atmosphere accounting for all coordinate directions; when having subscript 1 it refers to calculation via first-order structure functions, when having subscript 2 it refers to calculation via second-order methods. Use of the subscript 'a' refers to the calculation from aircraft data; the quantity H_a thus refers to the fact that aircraft data taken in cruise flight sample the variables in both the horizontal and the vertical, something evident from the chemical and potential temperature traces on the first polar ozone flights (Murphy *et al*. 1989, Tuck 1989); the subscript 'a' will be used exclusively for such data, invariably calculated by first order structure functions in this paper. The subscripts 'h' and 'v' appended to H will refer to the Hurst exponent calculated in the horizontal and vertical, respectively; H with no subscript refers to the value for the atmosphere generally. Tuck *et al*. (2004) argued that there were important correlations between $H_a(s)$ and $H_a(T)$ with measures of jet stream strength, where it was also shown that $H_a(N_2O) = 0.56 \pm 0.01$ for a true passive scalar (nitrous oxide, a conservative tracer) in the lower stratosphere, with no evidence of scale breaks in the log–log plots; at approximately 310 ppbv its presence could not possibly have affected the motion of the aircraft. This is the theoretical value of $H = 5/9$ predicted by generalized scale invariance, from the ratio of the horizontal (1/3) to the vertical (3/5) scaling exponents. We focus on the scaling behaviour of temperature, wind speed and relative humidity in the 'vertical' from some 261 dropsondes (Hock and Franklin 1999), released at about 13 km altitude from the Gulfstream 4SP aircraft. A 'horizontal' perspective, largely in the upper troposphere but with some in the lowermost stratosphere, is available from the permanent meteorological instruments on the parent aircraft. The data thus permit the extension of previous lower stratospheric ER-2 and WB57F work to the upper troposphere, with 'vertical' scaling through the depth of the troposphere. Because of telemetry gaps and noise spikes in the data, the scaling analyses of dropsonde results in Tuck (2008, 2010) were limited to the calculation of the conservation or Hurst exponent H; the intermittency exponent (C_1) and the Lévy exponent (α) were not obtained. The results are discussed in the light of previous work, and what can be deduced from the application of generalized scale invariance to the troposphere, in particular the vertical aspects. Note that the values of C_1 and α were estimated by theoretical formulae in Lovejoy *et al*. (2009a), and see Lovejoy *et al.* (2007) for the wind field from 24 sondes dropped during one flight. In the latter analysis, selected subsets of observations were used to demonstrate the absence of isotropic turbulence on any scale. It has further been shown that the concept of a stable layer, whether examined statically via the Brunt–Väisälä frequency for both moist and dry cases or dynamically via the Richardson number, needs re-examination when viewed in high resolution under statistical multifractal analysis of dropsonde observations (Lovejoy *et al*. 2008). An investigation into the vertical cascade structure of the atmosphere and how the flux and cascade analyses were affected

by the fact that the dropsonde outages showed statistical multifractal behaviour has been published recently (Lovejoy *et al*. 2009a); the transmission of the data stream from the falling, swinging and rotating sonde to the parent aircraft was affected by the turbulent structure of the wind field; at certain orientations the signal was too weak. The work presented here includes a statistical description of the fluctuations from 885 dropsondes from three winters, adding to the previous cascade and flux analyses made for one winter from 246 sondes (Lovejoy *et al*. 2009a), and extending the latitude range from 43° N to 60° N. The fluctuations and their statistical multifractal scaling exponents are the quantities likely to be most relevant to remote sounding retrievals, given their ability to generate representative statistics of fluctuations in both nadir and limb directions. An example shows the importance of such small-scale fluctuations in the retrieval context: the high water vapour variability found by Sparling *et al.* (2006). Loughner *et al.* (2007) considered specific horizontal scales selected from aircraft data for air quality sounding by satellite, for both the design of the hardware and of the retrieval software. This subject is later discussed in §4.

Scaling approaches are quite varied in the literature, with many seeking to describe variation in atmospheric variables with a single exponent, usually the Hurst exponent H or a variant of it. Koscielny-Bunde *et al.* (1998) and Syroka and Toumi (2001) examined surface temperature, while Toumi *et al.* (2001), Varotsos (2005) and Varotsos and Kirk-Davidoff (2006) studied the ozone column density. The interaction of clouds with radiation has been studied by Marshak *et al.* (1997) and Davis *et al.* (1997); cloud microphysics has been considered by Falkovich *et al.* (2002) and Falkovich and Pumir (2007); and there is a large literature concerning rainfall and hydrology originating with the much-cited work of Schertzer and Lovejoy (1987). Turbulence is a difficult subject and has been for over a century; it is not surprising that it continues to be controversial; see, for example, Frisch (1995) and Davidson (2004). In the atmosphere, it spans 15 orders of magnitude in spatial scale, from the mean free path to a great circle, and there exists no simple unifying language or formalism that is adequate. We consider the approaches that use the idea of turbulence laws as emergent properties to be promising ones.

Finally, it is necessary to mention what is sometimes seen as the surprising or even incredible expectation that a vertical scaling could be found in the atmosphere, given the variety of perceived scales in the troposphere, ranging from the boundary layer through meso- and synoptic scales to the three maxima in the global-scale subtropical jet stream of both Northern and Southern Hemispheres. It was not 'expected'; it is what resulted from the objective analysis of observations by a well-tried set of algorithms.

2. Methods

The NOAA Gulfstream 4SP aircraft (Aberson and Franklin 1999) is equipped as a research aircraft and has a GPS dropsonde capability. The GPS dropsondes have been described elsewhere (Hock and Franklin 1999); most of the flights here involved flight legs that were along a great circle or close to it. The flight duration was 7+ hr at pressure altitudes of 41 000–45 000 ft (12.5–13.1 km), during which time sondes numbering 20–30 were dropped. The sondes typically took about 800 s to splash down, recording data at 2 Hz. The horizontal displacement between the release and splashdown points for a sonde was in the range 12–15 km; the separation at splashdown was ≈30 m between pairs of sondes released simultaneously (Lovejoy *et al*. 2008).

The directly measured variables were analysed: temperature, wind speed and relative humidity at equal time intervals, also transformed by linear interpolation to equal intervals of geopotential height to allow for the deceleration of the falling sonde as it encountered progressively denser air. It has been shown that linear interpolation makes no significant difference to the analysis of the fluctuations, which is what we are concerned with here, although it may do so for spectral analysis and for the analysis of fluxes and cascades (Lovejoy *et al*. 2009a). The characteristics of the dropsonde are listed in table 1. The data from the meteorological instruments on the aircraft itself were analysed at 1 Hz. The time and position details of the flight legs used from the 10 flights are shown in table 2 and are mapped in figure 1. Note that comparison of the data between two simultaneously ejected dropsondes indicated that the errors were much smaller than those nominally given in the dropsonde specification, see Lovejoy *et al.* (2008), yielding, for example, temperature resolution of 0.01 K and horizontal wind resolution better than 0.1 ms^{-1} with a horizontal separation at splashdown of typically 30 m after falling 13 km.

Of the total of 261 sondes dropped in 10 flights, 15 were eliminated because of a variety of problems; of the remainder, 11 failed to record wind speed data. The composite variograms (Tuck *et al*. 2004) for temperature and relative humidity thus contain 246 vertical profiles, while that for wind speed contains 235. The dropsonde data are at 2 Hz, so on the time-based variograms, $\log_{10}(r) = 2$, for example, corresponds to a lag of 50 seconds; r is the lag parameter used in the scaling calculation; see, for example, Tuck (2010). The time-based data were also transformed to an altitude (geopotential height) base, since the sondes decelerated from a fall speed of $\sim$22 ms^{-1} at 12 km to $\sim$16 ms^{-1} at 6 km and to $\sim$11 ms^{-1} near the surface. In this case, the same quantity corresponds to a lag of about 1000 m. The first 15 s of each drop were omitted from the analysis to ensure that the temperature probe had equilibrated. The only records included in the pressure–temperature–humidity analysis were those with status codes of P00 and S00; all records with P10 and S10, telemetry errors in the pressure, temperature and humidity, were filtered out (Martin 2004). Data with 1 in the second place represent errors in the telemetry of the wind data, and these were also eliminated. The P indicates data taken prior to sonde release (used for calibration), while S represents data taken during the sounding phase. Among the 261 dropped, there were 8 pairs of sondes ejected simultaneously from the Gulfstream 4; they were very reproducible, a fact used in analyses of the anisotropy of turbulence (Lovejoy *et al*. 2007) and of the sparse fractal 'Russian doll' structure of stable and unstable layers under static, convective and dynamic criteria (Lovejoy *et al*. 2008). The calculation of specific humidity, required for the convective stability analysis, was made using the relation given in Richard *et al.* (2006). For details of quality control measures on the

Table 1. Characteristics of dropsonde.

	Operating range	Accuracy	Resolution	Time constant
Pressure (mbar)	20–1060	0.5	0.1	< 0.01 s
Temperature (°C)	−90–40	0.2	0.1	2.5 s at 20°C, 3.7 s at −40°C
Humidity (%)	0–100	2	0.1	0.1 s at 20°C, 10 s at −40°C
Wind (ms^{-1})	0–150	0.5	0.1	

Table 2. Times and locations of flight legs.

Date and take-off time	Type	Start time	End time	Start latitude (N)	Start longitude (W)	End latitude (N)	End longitude (W)
4 March 2004 17:54:57	Ascent	0	1008	21° 29′ 44″	158° 49′ 51″	22° 44′ 18″	160° 36′ 24″
	Horizontal	1009	15673	22° 44′ 22″	160° 36′ 30″	29° 43′ 44″	153° 32′ 25″
	Horizontal	16111	20993	30° 33′ 5″	152° 42′ 16″	23° 5′ 42″	156° 35′ 3″
	Descent	20994	23399	23° 5′ 35″	156° 35′ 5″	21° 19′ 28″	157° 55′ 38″
5 March 2004 18:38:20	Ascent	0	4546	21° 18′ 25″	157° 56′ 42″	23° 51′ 52″	159° 3′ 48″
	Horizontal	4547	14298	23° 51′ 58″	159° 3′ 52″	39° 10′ 30″	168° 12′ 1″
	Horizontal	14563	26443	39° 33′ 51″	168° 29′ 1″	59° 40′ 2″	151° 31′ 47″
	Descent	26444	28013	59° 40′ 10″	151° 31′ 44″	61° 10′ 4″	149° 59′ 31″
6 March 2004 20:11:57	Ascent	0	4428	61° 10′ 18″	149° 59′ 56″	59° 21′ 4″	147° 44′ 5″
	Horizontal	4429	11673	59° 20′ 58″	147° 43′ 57″	47° 32′ 34″	134° 30′ 26″
	Horizontal	11824	17222	47° 19′ 21″	134° 11′ 35″	38° 17′ 7″	122° 55′ 10″
8 March 2004 19:12:38	Ascent	0	5966	33° 49′ 28″	118° 9′ 34″	34° 14′ 41″	121° 25′ 2″
	Horizontal	5967	18535	34° 14′ 42″	121° 25′ 10″	33° 50′ 52″	150° 0′ 0″
	Horizontal	18679	24513	33° 32′ 48″	150° 0′ 0″	22° 50′ 31″	156° 38′ 27″
	Descent	24514	26352	22° 50′ 23″	156° 38′ 31″	21° 19′ 19″	157° 54′ 54″
9 March 2004 18:13:37	Ascent	0	4281	21° 18′ 25″	157° 56′ 31″	21° 25′ 36″	154° 35′ 17″
	Horizontal	4282	15567	21° 25′ 36″	154° 35′ 9″	38° 25′ 34″	154° 29′ 35″
	Horizontal	15812	25744	38° 42′ 55″	154° 19′ 22″	20° 19′ 44″	155° 49′ 36″
	Descent	25645	27913	20° 15′ 49″	155° 38′ 59″	21° 19′ 18″	157° 54′ 53″
11 March 2004 19:09:09	Ascent	0	5063	21° 19′ 31″	157° 56′ 25″	24° 6′ 17″	158° 5′ 24″
	Horizontal	5064	16619	24° 6′ 23″	158° 5′ 25″	46° 47′ 42″	160° 58′ 46″
	Horizontal	16925	28721	46° 12′ 53″	160° 52′ 6″	23° 20′ 6″	157° 39′ 58″
	Descent	28722	30755	23° 19′ 58″	157° 39′ 58″	21° 19′ 31″	157° 55′ 18″
2 March 2004 19:09:06	Ascent	0	4367	21° 19′ 31″	157° 56′ 21″	24° 15′ 12″	156° 36′ 37″
	Horizontal	4368	9932	24° 15′ 19″	156° 36′ 35″	35° 58′ 34″	151° 0′ 46″
	Horizontal	10134	27211	36° 25′ 29″	150° 45′ 50″	23° 2′ 12″	157° 1′ 30″
	Descent	27212	29406	23° 2′ 6″	157° 1′ 32″	21° 18′ 24″	157° 55′ 29″
13 March 2004 18:55:12	Ascent	0	4716	21° 18′ 25″	157° 56′ 10″	21° 8′ 39″	160° 17′ 5″
	Descent	10516	11957	18° 14′ 26″	166° 55′ 36″	17° 46′ 58″	167° 7′ 48″
	Descent	16365	17701	20° 29′ 55″	159° 9′ 21″	21° 19′ 20″	157° 54′ 56″
14 March 2004 19:04:09	Ascent	0	4597	21° 18′ 25″	157° 56′ 42″	22° 48′ 33″	154° 59′ 29″
	Horizontal	4598	15010	22° 48′ 37″	154° 59′ 22″	40° 0′ 23″	147° 24′ 34″
	Horizontal	15217	23916	40° 0′ 16″	147° 59′ 25″	23° 18′ 19″	156° 59′ 13″
	Descent	23917	26837	23° 18′ 12″	156° 59′ 15″	21° 19′ 18″	157° 54′ 58″

Note: The take-off time is UTC. The start and end times are seconds from take-off.

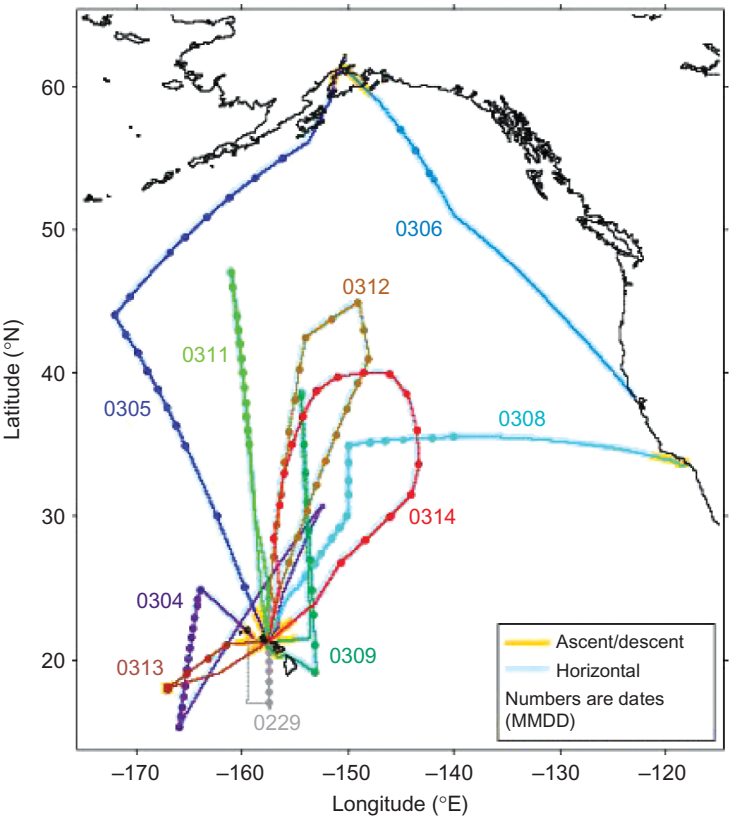

Figure 1. The flight tracks flown by the NOAA Gulfstream 4SP aircraft during the period 29 February 2004 to 14 March 2004. Dropsonde locations are indicated by the dots.

dropsonde data, the ASPEN Manual (Martin 2004) should be consulted. The altitude is the hydrostatically integrated altitude. The wind rejection algorithm uses the vertical velocity as measured by the GPS as an indicator of the reliability of the horizontal winds; if it is significantly different from the vertical velocity diagnosed from the pressure measurement, the GPS-reported horizontal winds are discarded.

It may be noted that the comparisons between simultaneously ejected sondes indicate that the errors are considerably smaller than the 0.5 ms^{-1} quoted, see Lovejoy *et al.* (2008). In any case, the best approach at the small scales is to include all the points and inspect the behaviour for consistency; see, for example, Tuck *et al.* (2003b) and Lovejoy *et al.* (2004). Most of the dropsondes encountered one or more wind maxima, which we classified as the subtropical, polar front and stratospheric polar night jet streams (STJ, PFJ and SPNJ, respectively). The SPNJ was encountered only when the aircraft was well above the tropopause and was limited to seven soundings, largely at the higher latitudes. The classification was based on a combination of altitude of wind speed maximum below the tropopause (above 10 km was STJ, below it was PFJ), continuity and a threshold wind speed above and below the wind maximum on each sounding. This threshold varied in the range 23–30 ms^{-1}; the distance between this threshold above and below the wind speed maximum was taken as the depth of the

jet stream. There was a sub-population of soundings having both STJ and PFJ occurrences on the same dropsonde record. For all the dropsonde profiles, a measure of the vertical shear of the horizontal wind was taken by calculating the difference between the maximum and minimum values of the wind speed recorded during the sounding. The entire set of 885 useable dropsonde profiles taken over three winters constitutes a new data set for the eastern Pacific Ocean between 15° N and 60° N and reinforces the previous analyses performed on smaller and less extensive samples, while dealing solely with the fluctuations in the observed variables, the quantities relevant to retrieval algorithms and their validation.

To calculate $H_{1,\mathrm{v}}$ via first-order structure functions for the dropsondes using an altitude base rather than a time base, the time series $f(t)$ was replaced by $f(z)$, where z is altitude and the data interval was 10 m. The individual variograms from which the time-based composites were made averaged 12 points each, resulting in approximately 2900 points in the composite variograms; the corresponding figure for the altitude-based analysis was 2600. The composites contain more points than an individual ascent by a factor approaching 2, because the individual descents are not perfectly aligned in either time or altitude and so the ∼1600 points taken at 2 Hz during ∼800 s fall time may fall in adjacent rather than identical bins. In what follows, we use the altitude-based variograms for the dropsonde data. The aircraft ascents, descents and cruise observations tend to be at constant rates of climb, dive and cruise and we use the directly acquired time-based method for the aircraft data. Sensitivity tests of these procedures indicated negligible effects on the results. We note that composite variograms are not limited to their familiar second-order usage in spectral analysis; here they are used with first-order structure functions, see the discussion in Tuck (2008, p. 43).

The theory for the analysis of atmospheric and geophysical data via generalized scale invariance has been given in several places in the literature, most recently in Lovejoy *et al.* (2010) and Tuck (2010). Some interest may attach to how our approach compares with that of other techniques of scaling analysis, such as rescaled range (Tuck and Hovde 1999) and in particular detrended fluctuation analysis (DFA; see Koscielny-Bunde *et al.* 1998) and its generalization, the Multifractal DFA (MFDFA). The fact that the dropsonde data are irregularly distributed in space forces resort to pairwise techniques (Lovejoy *et al*. 2007) and to a triplet technique both for the fluxes (to determine the cascade structure) and for the fluctuations, discussed in Lovejoy *et al.* (2009a), in which §4.4 contains details. The triplets are essentially a generalization of the MFDFA technique useful when the data are irregularly spaced. We therefore expect a DFA analysis to produce similar results for H_{v} to those in table 3(*b*).

3. Analysis of results

A typical dropsonde descent is shown in figure 2, with data for temperature, horizontal wind speed and relative humidity, accompanied by the individual height-based variograms from the slope of which $H_{1,\mathrm{v}}$ was calculated; consistent with the definitions given above, this refers to the Hurst exponent in the vertical calculated via first-order structure functions.

The descent occurs through the depth of the troposphere, at approximately 25° N and 157° W on 29 February 2004 (sonde number 1); the tropopause is visible at 12.5 km near the top of the temperature trace and was associated with the presence of a cut-off low (Cooper *et al*. 2005). It is immediately apparent that the 'vertical' scaling of temperature from the first-order structure functions has $H_{1,\mathrm{v}}(T)$ close to but less

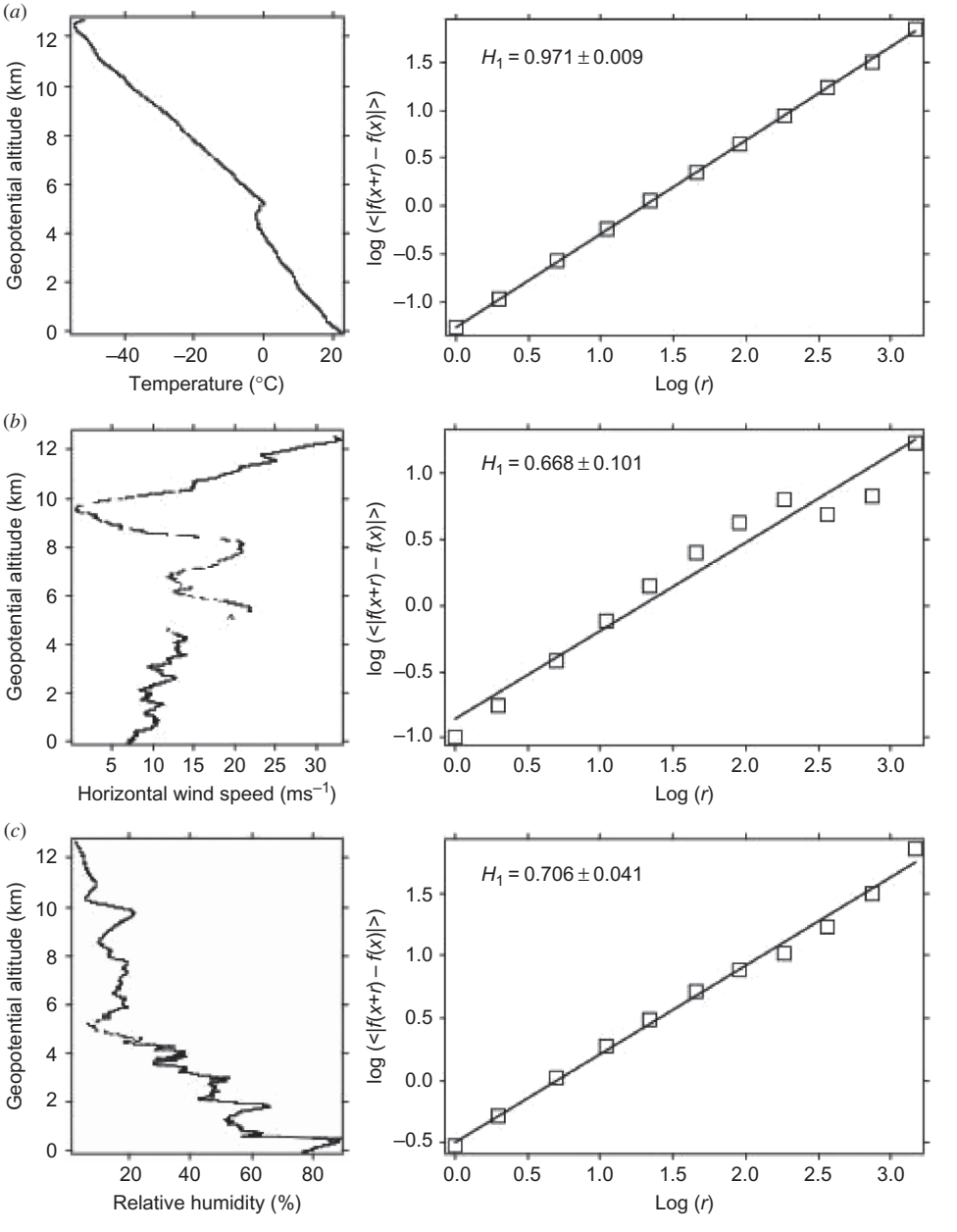

Figure 2. Dropsonde number 1, 29 February 2004; the location was 24° 57′ 01″ N, 157° 23′ 53″ W. The two frames in each of the three cases show the profile and its geopotential height-based variogram: (*a*) temperature; (*b*) wind speed; and (*c*) relative humidity. The scaling exponent $H_{1,v}$ is calculated from the slope of the variogram. The scaling in (*b*) is shown as an example of worst-case statistical variation at the large scales; more typical behaviour is shown in figures 3(*b*) and 4(*b*), with the composite behaviour of all the data in figure 5(*b*).

than unity, whereas $H_{1,v}(R)$ and $H_{1,v}(s)$ are approximately 0.7 and R is the relative humidity. The large deviations at the longer scales in figure 2(*b*) are shown to illustrate the worst case; the great majority of profiles are less scattered, as in figures 3(*b*) and 4(*b*).

There are of course fewer samples in the fractal analysis at the larger scales, but the effect is partially overcome in the composite variogram, see figure 5(*b*). Individual profiles at the latitudinal extremes of the dropsondes are shown in figures 3 and 4, in the shape of sonde number 17 on 05 March 2004 at 43° N and 171° W at the northernmost extent and sonde number 27 on 04 March 2004 at 15° N and 166° W at the southernmost extent of the sonde data. The data from these three sondes are very similar with regard to their scaling behaviour for temperature, wind speed and relative humidity and all deviate little from the composite variograms shown in figure 5, which include all the dropsonde data from all the flights. It should be noted that the tropopause on the northernmost sonde (figure 3) was well below the uppermost point (∼9 km vs. ∼12 km). Although all the temperature exponents are close to unity, as expected from the coarse persistent lapse rate present in tropospheric profiles, there is nevertheless an ordering within the range $0.91 < H_{1,v}(T) < 1.00$ according to variability, with the (rarer) profiles deviating most from a coarse straight lapse rate having lower values within the range. This is despite the choice of the absolute difference to define the fluctuation in the first-order structure function limiting the arithmetically possible range (theoretically $H_{1,v} \leq 1$). The variability is mainly that arising from 'stable' layers through the depth of the troposphere (Lovejoy *et al*. 2008). The approximately isothermal layer at the top of each sonde descent did tend to slightly lower the value of $H_{1,v}$ from unity, but in a very reproducible way, arising from the near constancy of both the tropopause and the aircraft flight altitudes. A second-order analysis of the 2004 data permitting a range of $H_{2,v}$ between 0 and 2 showed that $H_{2,v}(T) = 1.07 \pm 0.18$, with significant variability (Lovejoy *et al*. 2009a). The central point is that in both first- and second-order methods, the scaling of temperature fluctuations in the 'vertical' is different, with a higher H_v, than that of winds and humidity. The wind speed and humidity have similar scaling exponents in both first- and second-order results. With 'horizontal' observations, all three variables scale similarly, further supporting the uniqueness of the temperature fluctuations in the 'vertical'. Extensive tests and trials with a wide variety of algorithms support the interpretation of the calculated 'vertical' exponents as valid and significant.

The composite variograms – one calculation for the data points from all the flights rather than an average of the separate slopes – for the Gulfstream 4SP ascents and descents are shown in figure 6, and for the 'horizontal' segments in figure 7; the resulting scaling exponents H_a are shown in table 3; the data are consistent with the previous experience of 'horizontal' aircraft flight, with the H_a values being the ratio of the horizontal to the vertical scaling exponents (Lovejoy *et al*. 2004, Tuck 2008, Lovejoy *et al*. 2009b). The ascents and descents are mainly near Honolulu, with one of each above both Anchorage and Long Beach. The scaling is not significantly different for either of the latter locations. In figure 7(*c*), it should be recalled that total water has a sink, via gravitational settling of ice crystals, operative (Tuck 2008, 2010), thus rendering individual realizations different within the composite variogram, with sinks being indicated by $H_a < 5/9$. The effect is particularly pronounced at the longer scales. The line is simply the slope of all the data and represents a mean. It is clearer than having several lines corresponding to the individual flights.

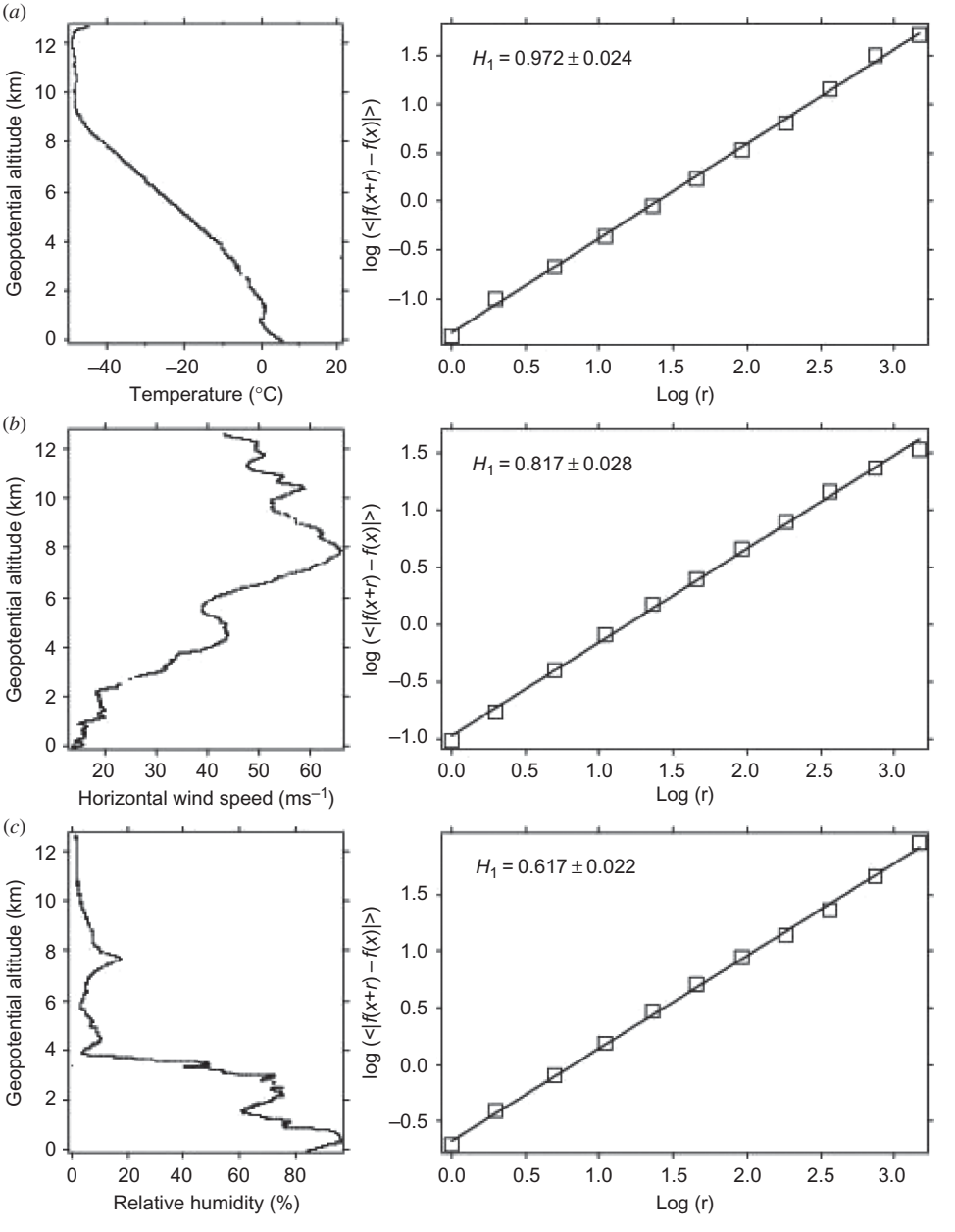

Figure 3. Northernmost dropsonde during the mission, number 17 on 5 March 2004 at 42° 42′ 56″ N, 170° 55′ 30″ W, as in figure 2.

In late January and early February 2004, the WB57F aircraft acquired 'vertical' profiles above San José Airport, Costa Rica (10° N, 84° W), where the tropopause was at an average altitude of 17 km (Richard *et al*. 2006) in the course of the pre-Aura Validation Experiment (pre-AVE). The composite variograms, which contain eight profiles, using a 1 Hz time base are shown for temperature and humidity in figure 8(*a*)

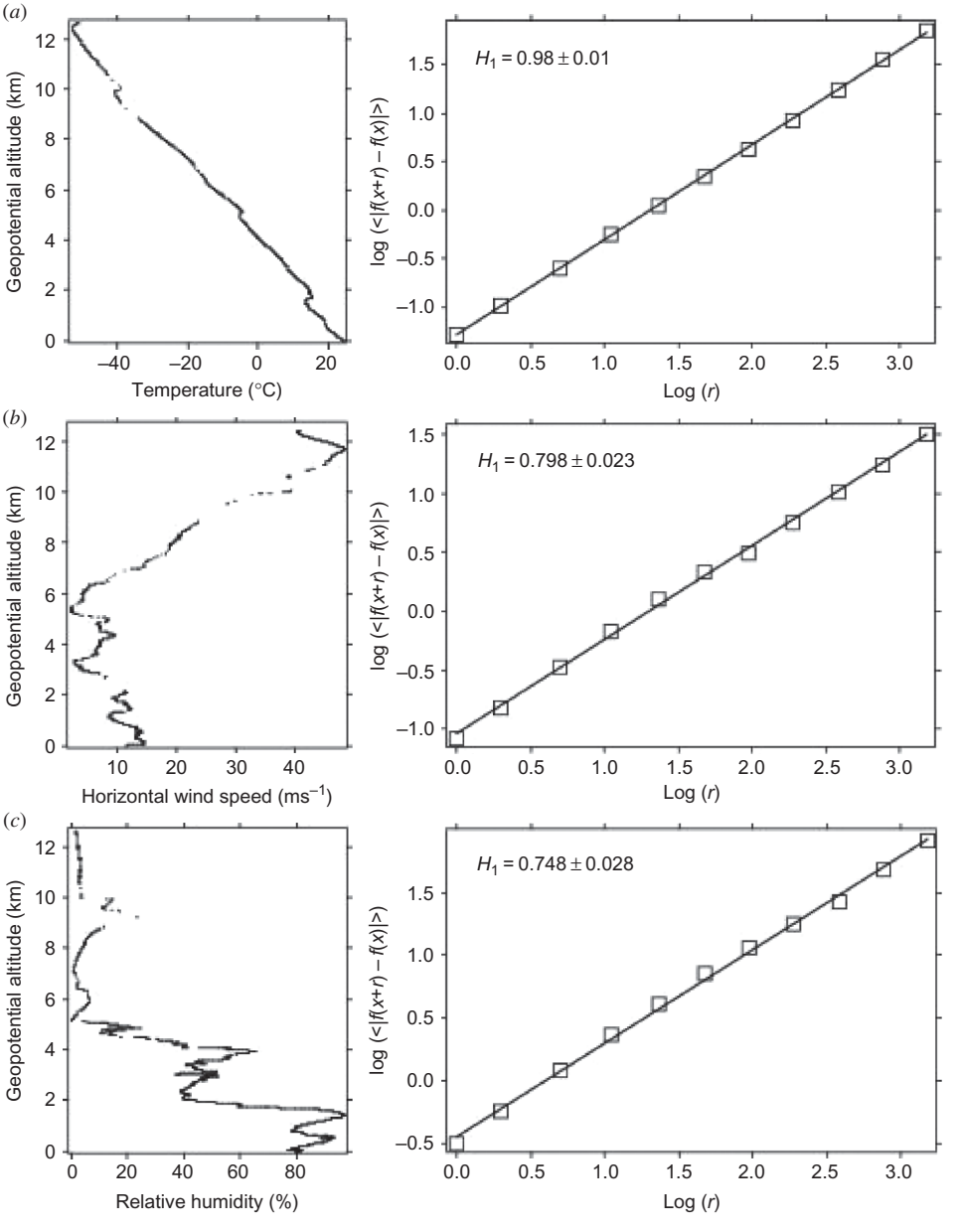

Figure 4. Southernmost dropsonde during the mission, number 27 on 4 March 2004 at 15° 15′ 11″ N, 165° 59′ 42″ W, as in figure 2.

and (*c*); they are not significantly different from those obtained by the Gulfstream 4SP at higher latitudes. Note that there were no research quality winds from the WB57F – those from the operational navigation system are inadequate for calculating $H_{1,v}(s)$, a point that may be seen from the slope and scatter in figure 8(*b*). The result provides a perspective on the requirements for systematic and random error to obtain useful scaling exponents; the quoted errors on the dropsonde data are adequate, as

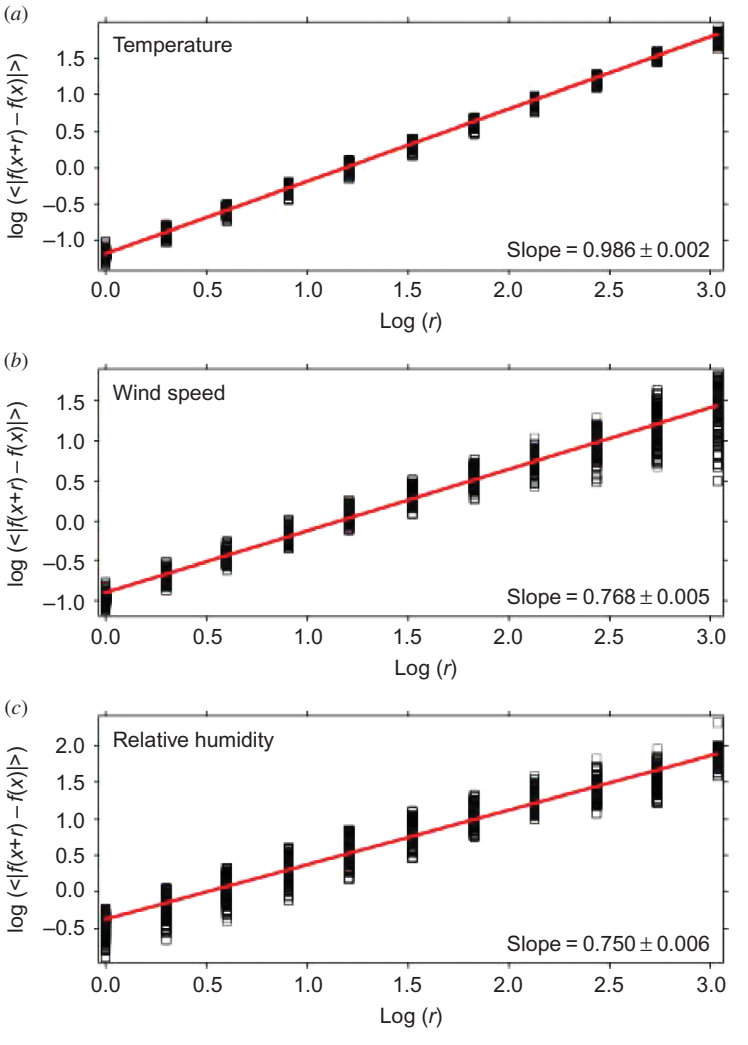

Figure 5. Composite variogram for all dropsondes during the mission: (*a*) temperature; (*b*) wind speed; and (*c*) relative humidity. See text for numbers of contributing sondes.

they were for the research data from the ER-2 and G4 aircraft, typically giving scaling exponents with standard errors of <10%. A similar experience was found with truncation error on archived, as contrasted to full double precision, data on the ER-2 (Tuck *et al*. 2002). There were no adequate 'horizontal' flight segments from pre-AVE. The 'vertical' flight segments of the WB57F were between the surface and 18 km altitude, typically taking between 15 and 20 minutes; four were ascents and four were descents. The similarity in the scaling between the 'vertical' ascents and descents, of the aircraft on one hand and of the dropsondes on the other, reinforces the validity of both, given the dissimilarity of the scaling of both to that of the aircraft data in the 'horizontal'.

The results from all the composite variograms from the first-order structure function analysis are summarized in table 3(*a*), which also contains for comparison in table 3(*b*) the values calculated by the second-order methods in Lovejoy *et al.* (2009a,b). The

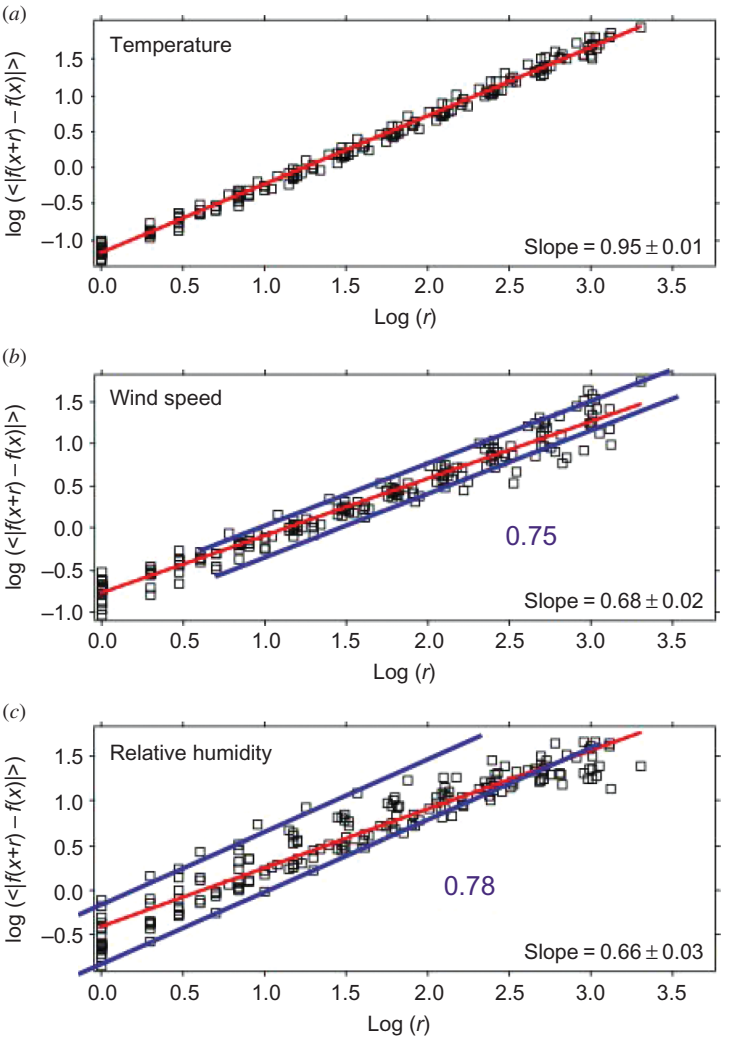

Figure 6. Composite variograms for the Gulfstream 4SP aircraft data ascents and descents, 18 profiles in all (see text): (*a*) temperature; (*b*) wind speed; and (*c*) relative humidity.

values for the 'vertical' scaling of temperature, wind speed and relative humidity from dropsondes are in the first column of table 3(*a*), with the corresponding values for aircraft ascents and descents (vertical) in the second column. The third column contains the 'horizontal' scaling exponents for the parent Gulfstream 4, which as noted previously combine horizontal and vertical fluctuations because of the effects of the turbulent structure upon the motion of the aircraft (Lovejoy *et al.* 2004, 2009b, 2010). Table 3(*b*), showing the second-order analysis, has the dropsonde results in the first column, the 'horizontal' aircraft results in the second and their ratio in the third.

There was no correlation of the 'vertical' scaling exponents $H_{1,v}(T)$ and $H_{1,v}(R)$ from the dropsonde data with either the depth of the jet streams or the magnitude of the vertical shears of the horizontal wind speed. There was, however, significant correlation of the vertical, dropsonde-derived $H_{1,v}(s)$ with these quantities for all three

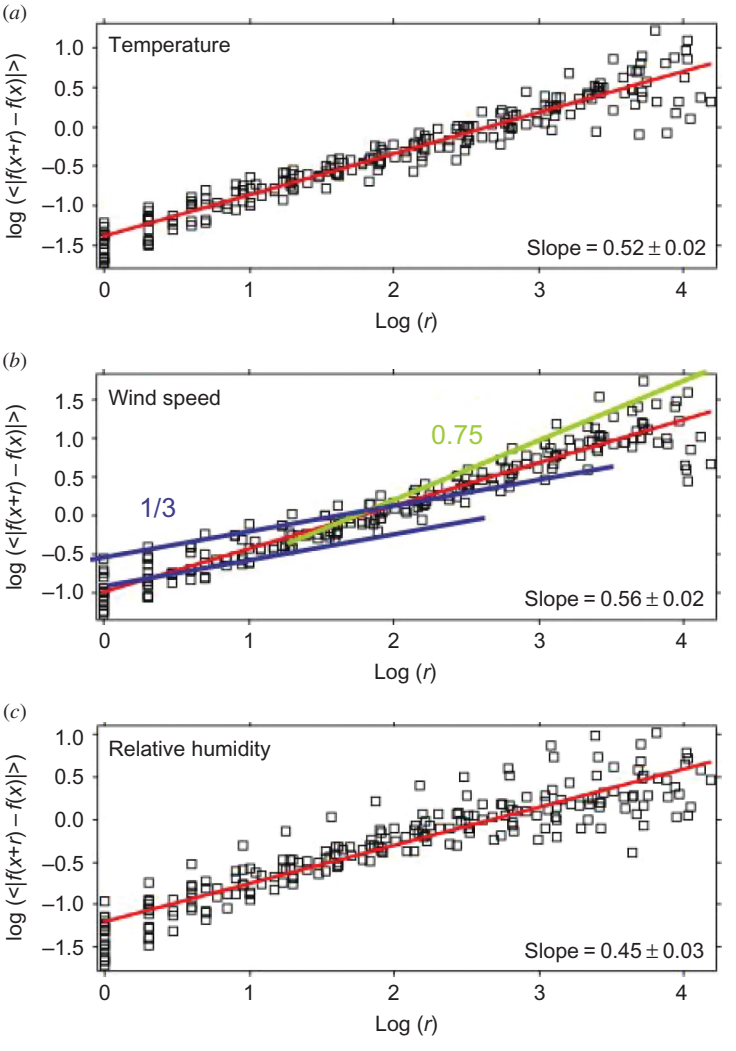

Figure 7. Composite variograms for the Gulfstream 4SP 'horizontal' segments (16 in all): (*a*) temperature; (*b*) wind speed; and (*c*) relative humidity.

categories of jet stream; see figure 9(*a*) for the correlation with depth of the jet stream. There is some separation of the STJ exponents from those of the polar front and SPNJ on this plot. Figure 9(*b*) shows a cleaner correlation of $H_{1,\mathrm{v}}(s)$ with the vertical shear of the horizontal wind, echoing that found in the 'horizontal' constant Mach number ER-2 data for the SPNJ (Tuck *et al*. 2004), with little evidence on separation among the three latitude bands. The important point is that traditional large-scale measures of jet streams, which are expressed theoretically in the thermal wind equation, are correlated with observed scaling exponents describing the fluctuations in the variability of the winds on all observed scales, in both horizontal and vertical. In Lovejoy *et al*. 2009a, somewhat different interpretation is given for the isobaric, parent G4 aircraft flight data: that at small scales before the G4 aircraft starts to accurately follow isobars, the horizontal wind exponent ($H_{\mathrm{h}} \approx 0.33$) is measured, while at large enough scales

Table (3*a*). Scaling exponents $H_{1,v}$ from dropsondes and H_a from the parent aircraft.

	Dropsondes	'Vertical' aircraft segments	'Horizontal' aircraft segments
Temperature	0.986 ± 0.002	0.95 ± 0.02	0.52 ± 0.02
Wind speed	0.768 ± 0.005	0.68 ± 0.02	0.56 ± 0.02
Relative humidity	0.750 ± 0.006	0.66 ± 0.03	0.45 ± 0.03

Table (3*b*). Scaling exponents $H_{2,v}$ from dropsondes and H_a from the parent aircraft (Lovejoy *et al*. 2009a,b).

	Dropsondes	'Horizontal' aircraft segments	H
Temperature	1.07 ± 0.18	0.50 ± 0.01	0.47 ± 0.09
Wind speed	0.75 ± 0.05	0.33 (1/3)	0.46 ± 0.05
Relative humidity	0.78 ± 0.07	0.51 ± 0.01	0.65 ± 0.06

the aircraft follows isobars which have significant slopes and the vertical exponent ($H_v \approx 0.75$) is measured. On any given trajectory, the transition distance is highly variable depending on the atmospheric condition (stability, shear) as well as on the aircraft response (autopilot, etc.), but on average is about 40 km. The result is that exponents estimated over scale ranges straddling the transition scale will have intermediate behaviours. The extreme horizontal and vertical exponents are shown as reference lines in the figures. Note that humidity and temperature were not strongly correlated with the aircraft altitude or pressure so that their exponents are not much affected by the atmospheric conditions. The foregoing complications do not apply to the dropsondes.

Figure 10(*a*) and (*b*) shows the grand average PDFs combining 2004, 2005 and 2006 for dropsonde temperature and relative humidity. Figure 11 shows the same grand average for dropsonde horizontal wind speed. All are non-Gaussian, including the lowest levels that are in the marine boundary layer, an important point to make for two reasons: one is that the point is made for a large area of the Pacific Ocean; and the second is that it makes the point that the Gaussian assumptions often made in atmospheric model procedures and variances, and in remote sounding retrievals, are inappropriate. Mean field assumptions will also require statistically correct justification, and account will need to be taken of the non-convergence of variances.

In order to enhance earlier results for 235 sondes from 2004 (Lovejoy *et al*. 2007), we show in figure 12 the vertical scaling behaviour of the horizontal wind speed for all 315 useable sondes from the 2006 mission, which extended the latitude range poleward to 60° N compared to the 43° N of the previous missions. The results are indeed similar to the earlier analysis although the previous results showed a systematic increase from $H_v \approx 0.60$ near the surface to ≈ 0.77 at altitude; here the range was 0.68–0.73.

Results were calculated for the intermittency, C_1, and the Lévy index, α, for the three directly measured variables – temperature, wind speed and humidity. The mean values were {0.072, 0.088, 0.091} for C_1 and {1.70, 1.90, 1.85} for α. Such values are

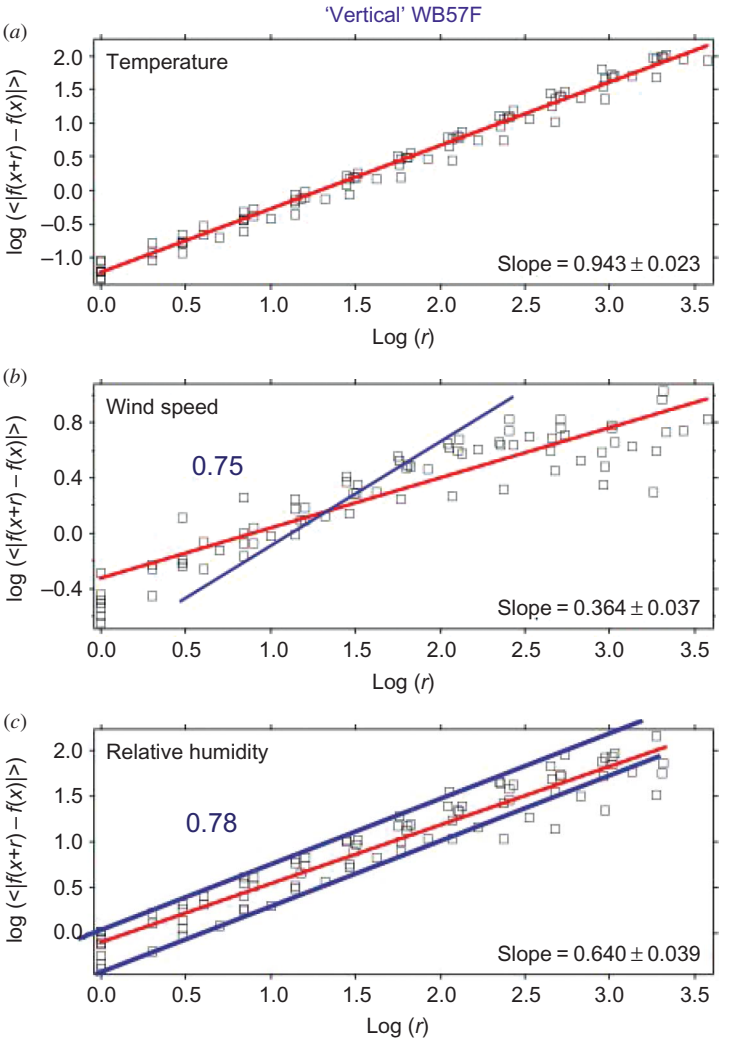

Figure 8. Composite variograms for ascents and descents of the WB57F during the pre-AVE mission above San José Airport, Costa Rica during late January and early February 2004: (*a*) temperature; (*b*) wind speed; and (*c*) relative humidity. The wind speed data are from the navigation system, not from research instrumentation, and are shown to illustrate the rather strict requirements on instrument performance and data quality that exist for the scaling analysis.

consistent with our previous work (Lovejoy *et al*. 2007, 2009a), where a more complete conceptual discussion of fluxes and cascades may be found. For all three variables, the large number of small samples at the short space and timescales in the scaling analysis overcomes the individual errors on a single observation. This is particularly true when considering the 885 profiles from the three winters, but is also effective in the case of the 246 sondes from 2004. In the particular case of relative humidity, the dropsonde values are better than those from operational radiosondes because they are taken on descent, so avoiding the contamination and outgassing problems entailed by ascent

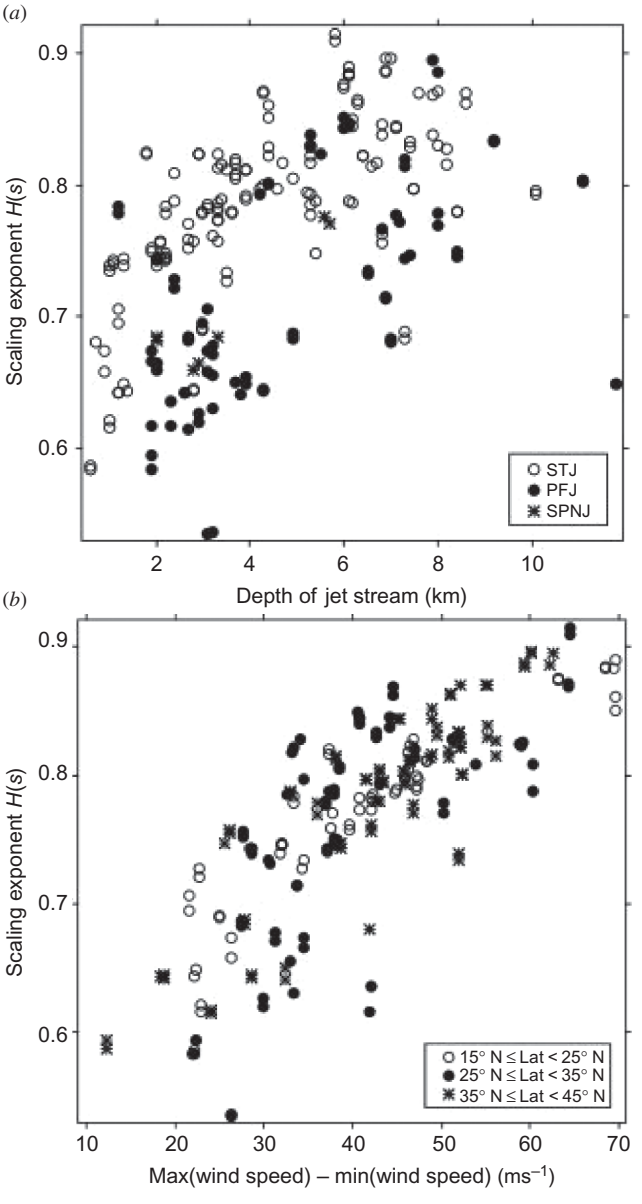

Figure 9. (*a*) The vertical scaling exponent $H_{1,v}(s)$ as a function of jet stream depth, obtained from dropsonde data. Open circles, STJ; closed circles, PFJ; asterisks, SPNJ (see text for definitions). (*b*) $H_{1,v}(s)$ versus the difference between the maximum and minimum wind speeds recorded on the sounding, a measure of the vertical shear of the horizontal wind. Open circles, latitudes 15° N–25° N; closed circles, latitudes 25° N–35° N; asterisks, latitudes 35° N–45° N.

from the surface. However, we have not been able to compare the relative humidities from the dropsonde with the independent absolute humidity measurements from the aircraft, because the sonde drops through a steep humidity gradient in the initial phase of its descent, when it is equilibrating thermally with the air after leaving the cabin.

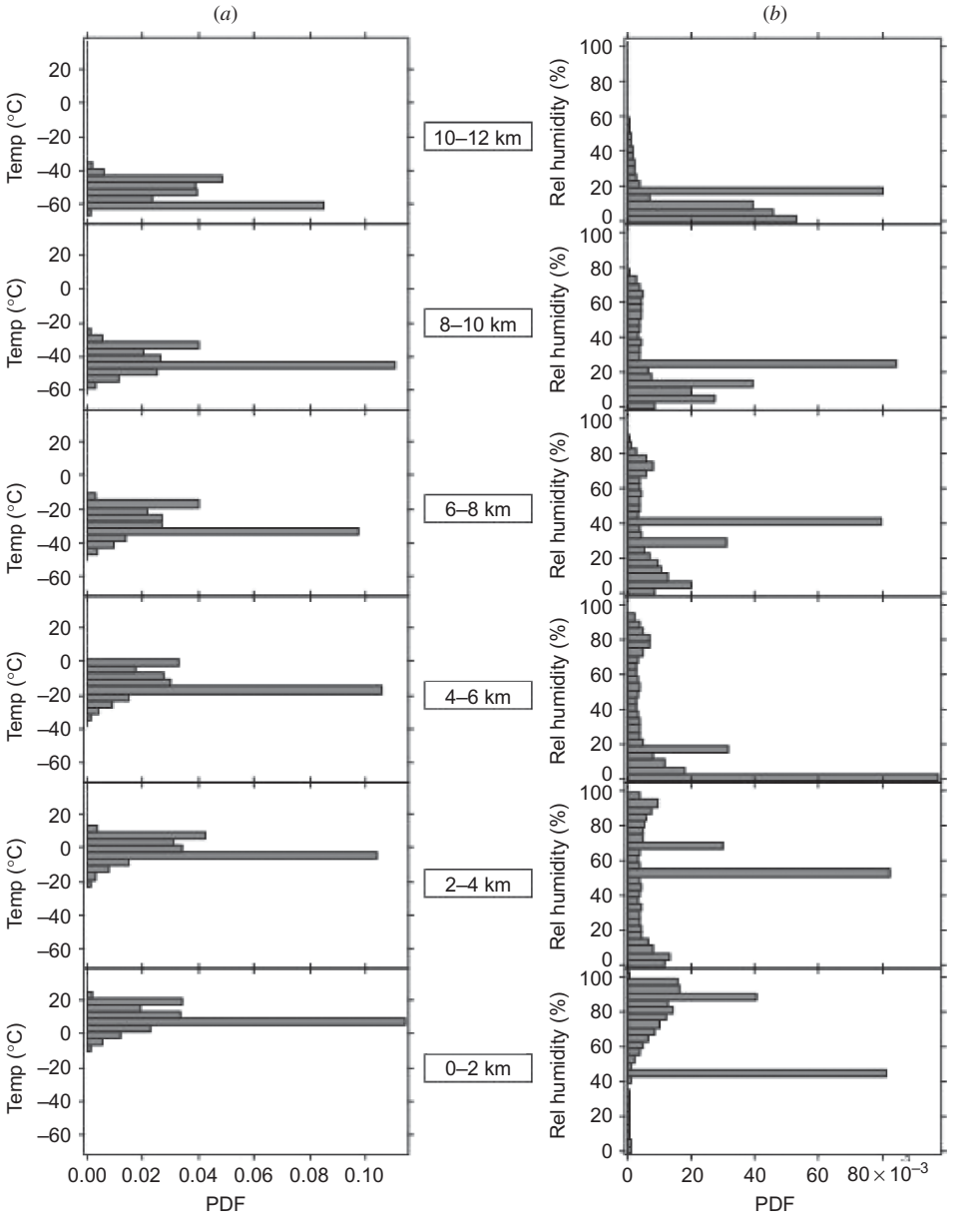

Figure 10. Total of 885 dropsondes from 2004, 2005 and 2006. The PDFs are shown for each 2 km deep layer from the surface to 12 km: (*a*) temperature; and (*b*) relative humidity.
Note: PDF, probability distribution function.

4. Discussion

We begin by noting that the observationally based generalized scaling exponents obtained here can be used to generate statistical multifractal data that will be representative of the troposphere above the Northern Hemisphere in the eastern Pacific Ocean in winter by the methods used, for example, in Lewis *et al.* (1999), Murphy

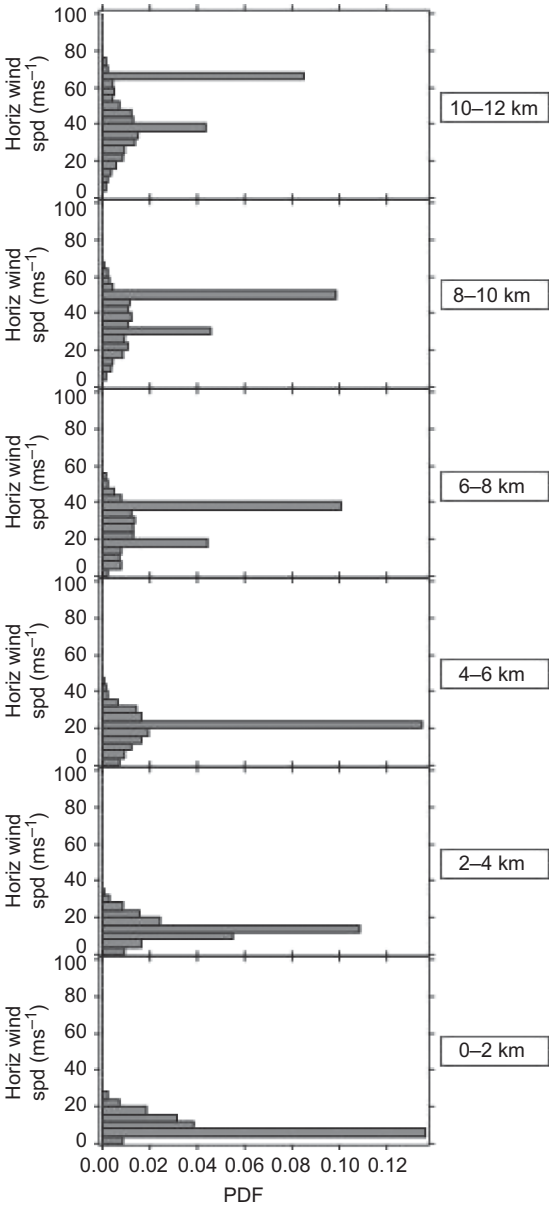

Figure 11. Total of 876 dropsondes from 2004, 2005 and 2006. The PDF of horizontal wind speed is shown for each 2 km layer from the surface to 12 km. Note: PDF, probability distribution function.

(2003), Tuck (2008) and Lovejoy and Schertzer (2010a,b). The importance of the vertical structure in the scaling behaviour of tropospheric temperature time series from satellite data has been shown recently by Efstathiou and Varotsos (2010), for example. The observations apply to a large area of the Pacific Ocean between the dateline and the west coast of North America, between 15° N and 60° N, with some ascents

and descents from the WB57F at 10° N between the surface and 18 km. The dropsonde and G4 results apply to the entire depth of the troposphere from the sea surface to 13 km in the 'vertical' and largely to the upper troposphere in the 'horizontal', in contrast to the earlier applications of scaling to high altitude research aircraft observations, which were very largely to lower stratospheric data in the 'horizontal' (Tuck *et al*. 2002, 2003a,b, 2004, 2005). The dropsonde data are more nearly vertical than the aircraft ascents and descents; nevertheless, the use of 'vertical' to describe the aircraft ascents and descents out of and into airports is justified by the scaling behaviour. Although it has been demonstrated that the trajectories of the ER-2 and G4 aircraft under autopilot control can themselves be fractal (Lovejoy *et al*. 2004, 2009b, 2010),

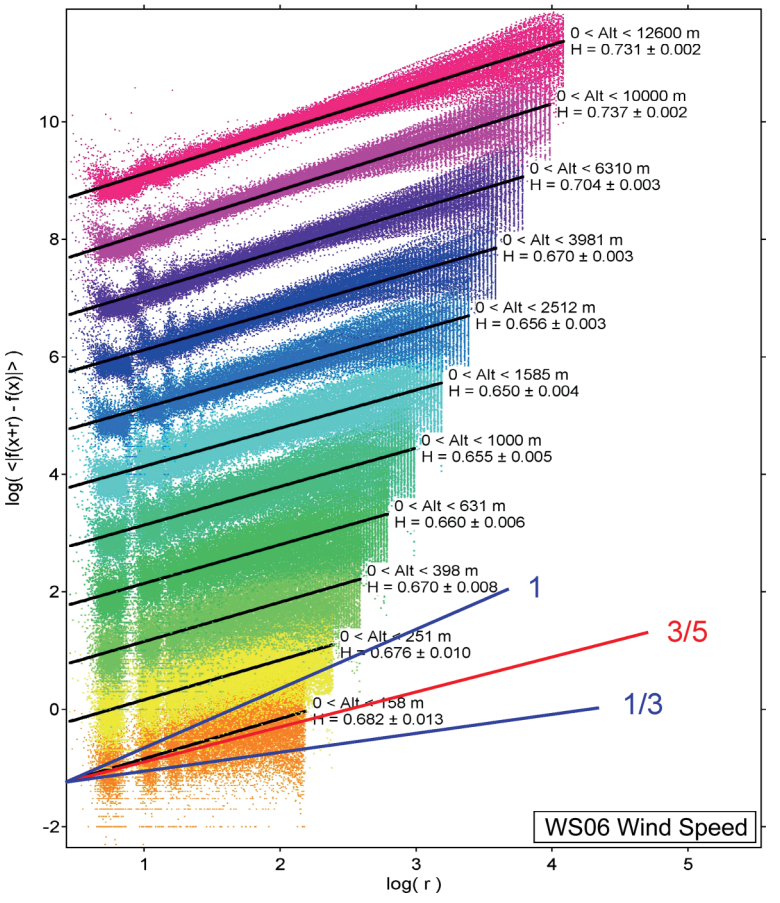

Figure 12. Total of 315 dropsondes dropped during Winter Storms 2006, in the area 21°N–60° N, 128° W–172° W. The vertical scaling of the horizontal wind is shown. The fits are rms to the vertical shears across layers of thickness increasing logarithmically upwards. The reference lines have slopes corresponding to $H_v = 1$ (gravity waves), $H_v = 3/5$ (BO) and 1/3 (Kolmogorov). The H_v corresponding to each rms fit is given. The data for each level are offset by 1 order of magnitude to aid legibility. While BO is a good fit in the lower troposphere, in the upper troposphere the presence of jet streams leads to a systematic increase when the upper troposphere is included. In any event, isotropic turbulence is always precluded. See Lovejoy *et al.* (2007) and Tuck (2008). Note: rms, root mean square; BO, Bolgiano–Obukhov.

the similarity of the H_1 scaling exponent for the 'vertical' structure in temperature, relative humidity and wind speed measured from the dropsondes and measured from the G4 aircraft during ascents and descents suggests that the motion of the platform is not a major influence in this regard, in particular the effect of the horizontal displacement during the sonde descents is small. Platform motion is significant, however, for isobaric G4 aircraft wind data in 'horizontal' flight when attempting flux and cascade analyses, which have been given elsewhere (Lovejoy *et al*. 2009b, 2010). The key effect noted in the latter paper was that when the aircraft attempted to follow isobars, there was a critical transition scale. Below that scale, pressure fluctuations trailed the wind fluctuations, whereas at larger scales they led them. Since the isobars generally have significant slopes with respect to the vertical, and the turbulence is anisotropic, the isobaric wind exponents are equal to the vertical wind exponents, not the horizontal (isoheight) wind exponents.

According to the theory of generalized scale invariance (Schertzer and Lovejoy 1985, 1987, 1991), one does not expect the exponents of the turbulence in the vertical and horizontal to be equal, so that structures become increasingly stratified at larger and larger scales. In the original application of the idea to the atmosphere, the ratio of the horizontal (H_h) to vertical (H_v) conservation scaling exponents H was argued to have the value 5/9, consisting of the ratio $1/3 \div 3/5$. The value of 1/3 in the horizontal originated with Kolmogorov (1962, 1991) and the 3/5 in the vertical with Bolgiano (1959); they result from the dimensional analysis applied to the horizontal energy flux (units $m^2\ s^{-3}$) and the vertical buoyancy flux (units $m^2\ s^{-5}$), respectively. The 'vertical' exponents are greater than the Bolgiano–Obukhov (BO) value for the horizontal wind (3/5) for both dropsonde and aircraft data, being near but significantly less than unity for temperature and about 0.75 and 0.68 for both relative humidity and wind speed (table 3(*a*)); see table 3(*b*) for the somewhat different values found in Lovejoy *et al.* (2009a) from a second-order analysis including the ratios H which are not far from 5/9 but are apparently somewhat different. The 'horizontal' scaling exponents for the aircraft data are 0.52, 0.56 and 0.45 for temperature, wind speed and relative humidity, respectively. The generalized scale invariance analysis of the vertical structure of the horizontal wind speed by Schertzer and Lovejoy (1985) found $H_v \approx 0.60$ using spectral analyses and $H_v = 0.50 \pm 0.05$ from probability distribution analyses of the ascent phase of 287 radiosonde launches, truncated to include only data up to 13 km altitude. This contrasts with our value from 235 dropsondes of 0.768 ± 0.005 for an almost identical altitude range. It is known that balloon payloads are in the turbulent wake of the balloon on ascent from the behaviour of the water vapour sensor, even when attached on long cables, so that data are completely reliable only on descent. This is less true of ozone and temperature, but may have affected the analysis of earlier stratospheric ascent data, for example, Tuck *et al*. (1999); we therefore suggest that the dropsonde data are more credible. Recent re-examination by Lovejoy of the Lazarev *et al.* (1994) radiosonde data suggests that the value of $\beta = 2.4$ works as well as the originally reported value $\beta = 2.2$, where β is the power spectral exponent, corresponding to $H_v = 0.75$ (including the small intermittency corrections).

The behaviour of upper tropospheric aircraft observations of humidity has been discussed previously, with the conclusion that in both hemispheres air was dried by cooling during sloping the motion up isentropes to the west of anticyclones (ridges) in the subpolar regions and to their east in the subtropics (Kelly *et al*. 1991, Yang and Pierrehumbert 1994); scaling behaviour indicated that total water was not a passive scalar (conservative tracer) in the subtropical case (Tuck *et al*. 2003b) or from the

DC-8 aircraft in the polar case (Tuck 2008). Galewsky *et al*. (2005) have confirmed this drying mechanism for the largest scales globally in the subtropics through the study of both re-analysis and general circulation model fields. The departure from passive scalar behaviour for humidity is not therefore surprising. The correlation of values of H_a less than, equal to and greater than 5/9 (0.56) with sinks, conserved tracers and sources for atmospheric molecules, respectively, has been discussed by Tuck (2008, 2010). An independent method for detecting the presence of sources and sinks for molecular species, including water, methane, carbon dioxide and ozone could be of great utility in remote sounding studies of radiatively active gases. One would, for example, expect to find a source of water in the lower altitudes in anticyclones above the subtropical oceans, where evaporation exceeds precipitation.

The 'vertical' scaling of temperature from the dropsondes ($1.00 > H_{1,v} > 0.91$) calculated from the first-order structure function is distinctly different from that of wind and humidity, which are essentially the same, about 0.75, whether calculated by first- or second-order methods (table 3). That the vertical exponents exist is significant, in that scaling is respected, but their numerical values are somewhat different from the theoretical expectation predicted by the simplest generalized scale invariance model with the BO exponent in the vertical and the Kolmogorov (K) value in the horizontal; this generalized scale invariance model predicts $H_h = H\,H_v$ with $H = 5/9$; Lovejoy *et al.* (2009a) found the estimates of H in the range 0.46–0.65 depending on the field. The aircraft ascents and descents have some small horizontal components, and while this is reflected in the slightly ($\leq$10%) lower 'vertical' exponents for all three variables, they basically confirm the dropsonde results, as do independent WB57F profiles taken for temperature and humidity through the depth of the tropical troposphere during pre-AVE (figure 8(*a*) and (*c*)). The grand average results presented here underline the weakness of Gaussian assumptions about the PDFs often assumed to apply to atmospheric variables and their variances in numerical models, and in retrieval algorithms in remote sounding. Sparling (2000) has pointed out the relevance of such PDFs to remote sounding of the stratosphere. The scaling exponents we provide offer the possibility of generating statistically representative fluctuations along remote sounding paths, in both nadir and limb geometries. In both cases they are not normally distributed, having long tails in their probability distributions; furthermore, the variances will not converge since the Lévy exponent $\alpha < 2$.

While scaling is still respected in the 'vertical', for both dropsonde and aircraft data, we have no explanation for the observed deviations of the numerical values of the exponents or the apparently significant deviations of the ratios from those predicted by the simplest generalized scale invariance model using the BO and K values, which has hitherto been successful in accounting for the scaling behaviour observed in 'horizontal' flight in the lower stratosphere (Lovejoy *et al*. 2001, 2004, Tuck *et al*. 2002, 2003a,b, 2004, 2005). Nevertheless, the calculated exponents H, C_1 and α do support the statistical multifractality predicted by generalized scale invariance and so demonstrate the importance of intermittency and non-Gaussianity.

The impact of small-scale variability in the 'horizontal' from aircraft data on the design and retrievals for satellite sounding of air quality has been considered by Loughner *et al.* (2007). They selected the typical length scales of approximately 50 km in the boundary layer, rising to approximately 150 km above it, and pointed out that 10 km resolution was needed to resolve horizontal variability in the column integral with its 50 km scale; the column integral is what is retrieved for many chemical species. While agreeing that the proper statistical characterization of small-scale fluctuations

is important in this context, we emphasize that we find statistical multifractal scale invariance. In the 'vertical', we see no difference in the scaling between the marine boundary layer and the free troposphere, but the scaling exponent H_v for wind speed does increase in the upper troposphere, showing correlations with jet stream properties, as does H_h in the 'horizontal'. A further feature of our analysis is that it finds numerical model-independent evidence as to whether molecular species, including water, have values of H that are characteristically showing source ($H>5/9$), tracer ($H = 5/9$) and sink ($H<5/9$) behaviours, something of potential utility in the study of radiatively active species such as methane and carbon dioxide for surface sources and sinks through their column abundance (Schneising *et al*. 2008, 2009), in addition to water in all its phases and the photochemically active molecules such as ozone.

5. Conclusions

The 'vertical' scaling of temperature fluctuations from hundreds of dropsondes and the 'vertical' scaling of temperature fluctuations from the aircraft ascents and descents are in both cases significantly different from the fluctuations of wind speed and humidity; this presumably demonstrates the overwhelming influence of gravity in this coordinate. The 'vertical' results for the scaling of all three variables are similar between the sondes and the aircraft, while the 'horizontal' data from the aircraft scale are significantly different from those in the 'vertical'. The results apply throughout the depth of the troposphere over a large area of the eastern Pacific Ocean of the Northern Hemisphere. However, deviations from hydrostatic equilibrium under gravity, although small, are significant. The coarse result is consistent with basic derivations from both microscopic (e.g. Moelwyn-Hughes 1961) and macroscopic (e.g. Gill 1982) points of view, resulting in a vertical conservation scaling exponent, $H_{1,v}(T)$, close to but significantly less than unity. A second-order analysis yields $H_{2,v}(T) = 1.07 \pm 0.18$. The deviations are small but significant, the associated vertical accelerations being variable and intermittent ($C_1 \approx 0.2$).

The scaling behaviour in the vertical of the wind speed shows significant correlation with both jet stream depth and vertical shear: a result paralleling the previously reported behaviour (Tuck *et al*. 2004) in the horizontal in which a link emerges naturally between the small-scale turbulent structure and the large-scale dynamics as manifested in jet streams (Tuck 2008, 2010).

The 'vertical' results from the dropsondes for relative humidity and wind speed have values of $H_{1,v}$ which are larger than the 3/5 predicted by the generalized scale invariance theory and for which to our knowledge no reasonable explanation exists. For the aircraft data, these were consistent with the sondes in the 'vertical' and showed that scaling pertains, ratios of the 'horizontal' to the 'vertical' exponents being approximately 5/9, within the limits of the measurements and corrections for aircraft motion shown in Lovejoy *et al.* (2004) – which is the theoretical value from the generalized scale invariance (Schertzer and Lovejoy 1985, 1987, 1991). The basic statistical multifractal scaling is respected well enough that the vertical flux and cascade structure is calculable and has been reported elsewhere (Lovejoy *et al*. 2009a). Isotropic turbulence, in the sense of 'vertical' scaling exponents like those in the 'horizontal', is never seen in this large data set, which is distributed over a wide area of the eastern Pacific in the Northern Hemisphere, reinforcing earlier conclusions from a smaller and more localized sample (Lovejoy *et al*. 2007). The mean values from the dropsondes of the statistical multifractal 'vertical' exponents H_v, C_1 and α

for temperature, wind speed and humidity were $H_{1,v}\{0.986, 0.768, 0.750\}$, $C_1\{0.072, 0.088, 0.091\}$ and $\alpha\{1.70, 1.90, 1.85\}$, respectively. These average values of the three scaling exponents provide a source describing the statistical characteristics of the 'vertical' structure of the fluctuations of temperature, wind speed and humidity in the marine atmosphere throughout the troposphere, which can serve as a generator of representative probability distributions for retrievals of remotely sounded observations. Since they correspond to statistical multifractal character, these probability distributions are non-Gaussian, with long tails corresponding to power-law behaviour. Like their 'horizontal' counterparts, they are scale invariant, vitiating the selection of particular scales, either horizontal or vertical, in the design of satellite instruments and their retrieval algorithms; further, variances do not converge. Humidity shows model-independent evidence for the presence of sinks, a feature of the H exponent that could be potentially useful if extended to source/sink analysis of column amounts of long-lived, radiatively active gases such as methane and carbon dioxide.

Acknowledgements

The efforts of the aircrew and staff of the NOAA Aircraft Operations Center are greatly appreciated. We are grateful to the National Weather Service and M. Shapiro for provision of a significant fraction of the flight hours and dropsondes as part of the Winter Storms 2004 Project. We thank O. Cooper, G. Hübler, D. Parrish, E. Ray, K. Rosenlof and D. Sueper of the then NOAA Aeronomy Laboratory, now the Chemical Sciences Division of the NOAA Earth System Research Laboratory, for help with flight planning and instrument installation.

References

Aberson, S.D. and Franklin, J.L., 1999, Impact on hurricane track and intensity forecasts of GPS dropwindsonde observations from the first season flights of the NOAA Gulfstream-IV jet aircraft. *Bulletin of the American Meteorological Society*, **80**, pp. 421–427.

Bolgiano, R., 1959, Turbulent spectra in a stably stratified atmosphere. *Journal of Geophysical Research*, **64**, pp. 2226–2229.

Cooper, O.R., Stohl, A., Hübler, G., Hsie, E.Y., Parrish, D.D., Tuck, A.F., Kiladis, G.N., Oltmans, S.J., Johnson, B.J., Shapiro, M., Moody, J.L. and Lefohn, A.S., 2005, Direct transport of mid-latitude stratospheric ozone into the lower troposphere and marine boundary layer of the tropical Pacific Ocean. *Journal of Geophysical Research*, **110**, D23310, doi: 10.1029/2005JD005783.

Davidson, P.A., 2004, *Turbulence* (New York: Oxford University Press).

Davis, A.B., Marshak, A., Cahalan, R.F. and Wiscombe, W.J., 1997, Solar and laser beams, stratus clouds, fractals and multifractals in climate and remote sensing studies. *Fractals-Interdisciplinary Journal of Complex Geometry in Nature*, **5**, pp. 129–166.

Efstathiou, M.N. and Varotsos, C., 2010, On the altitude dependence of the temperature scaling behaviour at the global troposphere. *International Journal of Remote Sensing*, **31**, pp. 343–349.

Falkovich, G., Fouxon, A. and Stepanov, M.G., 2002, Acceleration of rain initiation by cloud turbulence. *Nature*, **419**, pp. 151–154.

Falkovich, G. and Pumir, A., 2007, Sling effect in collisions of water droplets in turbulent clouds. *Journal of the Atmospheric Sciences*, **64**, pp. 4497–4505.

Frisch, U., 1995, *Turbulence: The Legacy of A. N. Kolmogorov* (New York: Cambridge University Press).

Galewsky, J., Sobel, A. and Held, I., 2005, Diagnosis of subtropical humidity dynamics using tracers of last saturation. *Journal of the Atmospheric Sciences*, **62**, pp. 3353–3367.

Gill, A.E., 1982, *Atmosphere – Ocean Dynamics, Vol. 30*, *International Geophysics Series* (San Diego, CA: Academic Press).

Hock, T.F. and Franklin, J.L., 1999, The NCAR GPS dropwindsonde. *Bulletin of the American Meteorological Society*, **80**, pp. 406–420.

Kelly, K.K., Tuck, A.F. and Davies, T., 1991, Wintertime asymmetry of upper tropospheric water between the Northern and Southern Hemispheres. *Nature*, **353**, pp. 244–247.

Kolmogorov, A.N., 1962, A refinement of previous hypotheses concerning the local structure of turbulence in a viscous incompressible fluid at high Reynolds number. *Journal of Fluid Mechanics*, **13**, pp. 82–85.

Kolmogorov, A.N., 1991, English translations of Kolmogorov's 1941 papers. *Proceedings of the Royal Society of London, Series A*, **434**, pp. 9–17.

Koscielny-Bunde, E., Bunde, A., Havlin, S., Roman, H.E., Goldreich, Y. and Schellnhuber, H.-J., 1998, Indication of a universal persistence law governing atmospheric variability. *Physical Review Letters*, **81**, pp. 729–732.

Lazarev, A., Schertzer, D., Lovejoy, S. and Chigirinskaya, Y., 1994, Unified multifractal atmospheric dynamics tested in the tropics: part II, vertical scaling and generalized scale invariance. *Nonlinear Processes in Geophysics*, **1**, pp. 115–123.

Lewis, G.M., Lovejoy, S., Schertzer, D. and Pecknold, S., 1999, The scale invariant generator technique for quantifying anisotropic scale invariance. *Computers and Geosciences*, **25**, pp. 963–975.

Loughner, C.P., Lary, D.J., Sparling, L.C., Cohen, R.C., Decola, P. and Stockwell, W.R., 2007, A method to determine the spatial resolution required to observe air quality from space. *IEEE Transactions on Geosciences and Remote Sensing*, **45**, pp. 1308–1314.

Lovejoy, S. and Schertzer, D., 2007, Scaling and multifractal fields in the solid earth and topography. *Nonlinear Processes in Geophysics*, **14**, pp. 45–502.

Lovejoy, S. and Schertzer, D., 2010a, On the simulation of continuous in scale universal multifractals. Part I: spatially continuous processes. *Computers and Geosciences*, **36**, pp. 1393–1403.

Lovejoy, S. and Schertzer, D., 2010b, On the simulation of continuous in scale universal multifractals. Part II: space-time processes and finite corrections. *Computers and Geosciences*, **36**, pp. 1404–1413.

Lovejoy, S., Schertzer, D. and Stanway, J.D., 2001, Direct evidence of multifractal cascades from planetary scales down to 1 km. *Physical Review Letters*, **86**, pp. 5200–5203.

Lovejoy, S., Schertzer, D. and Tuck, A.F., 2004, Fractal aircraft trajectories and nonclassical turbulent statistics. *Physical Review E*, **70**, 03630, doi:10.1103/PhysRevE.70.036306.

Lovejoy, S., Tuck, A.F., Hovde, S.J. and Schertzer, D., 2007, Is isotropic turbulence relevant in the atmosphere? *Geophysical Research Letters*, **34**, L15802, doi:10.1029/2007GL029359.

Lovejoy, S., Tuck, A.F., Hovde, S.J. and Schertzer, D., 2008, Do stable atmospheric layers exist? *Geophysical Research Letters*, **35**, L01802, doi:10.1029/2007GL032122.

Lovejoy, S., Tuck, A.F., Hovde, S.J. and Schertzer, D., 2009a, The vertical cascade structure of the atmosphere and multifractal dropsonde outages. *Journal of Geophysical Research*, **114**, D07111, doi: 10.1029/2008D010651.

Lovejoy, S., Tuck, A.F. and Schertzer, D., 2010, Horizontal cascade structure of atmospheric fields determined from aircraft data. *Journal of Geophysical Research-Atmospheres*, **115**, D13105, doi: 10.1029/2009JD013353.

Lovejoy, S., Tuck, A.F., Schertzer, D. and Hovde, S.J., 2009b, Reinterpreting aircraft measurements in anisotropic scaling turbulence. *Atmospheric Chemistry and Physics*, **9**, pp. 5007–5025.

Macdonald, A.E., 2005, A global profiling system for improved weather and climate prediction. *Bulletin of the American Meteorological Society*, **86**, pp. 1747–1764.

Marshak, A., Davis, A., Wiscombe, W. and Cahalan, R.F., 1997, Scale invariance in liquid water distributions in marine stratocumulus. Part 2: multifractal properties and intermittency issues. *Journal of Atmospheric Sciences*, **54**, pp. 1423–1444.

Martin, C., 2004, *ASPEN User Manual* (Boulder, CO: National Center for Atmospheric Research).

Moelwyn-Hughes, E.A., 1961, *Chapter 1 in Physical Chemistry*, 2nd Rev ed. (Oxford: Pergamon Press).

Murphy, D.M., 2003, Dehydration in cold clouds is enhanced by a transition from cubic to hexagonal ice. *Geophysical Research Letters*, **30**, p. 2230.

Murphy, D.M., Tuck, A.F., Kelly, K.K., Chan, K.R., Loewenstein, M., Podolske, J.R. and Strahan, S.E., 1989, Indicators of transport and vertical motion from correlations between in situ measurements in the Airborne Antarctic Ozone experiment. *Journal of Geophysical Research*, **94**, pp. 11669–11685.

Richard, E.C., Tuck, A.F., Aikin, K.C., Kelly, K.K., Herman, R.L., Troy, R.F., Hovde, S.J., Rosenlof, K.H., Thompson, T.L. and Ray, E.A., 2006, High resolution airborne profiles of CH_4, O_3 and water vapor near tropical Central America in late January–early February 2004. *Journal of Geophysical Research*, **111**, D13304, doi: 10.1029/2005JD006513.

Schertzer, D. and Lovejoy, S., 1985, The dimension and intermittency of atmospheric dynamics, In *Turbulent Shear Flows*, B. Launder (Ed.), pp. 7–33 (New York: Springer-Verlag).

Schertzer, D. and Lovejoy, S., 1987, Physical modeling and analysis of rain and clouds by anisotropic scaling multiplicative processes. *Journal of Geophysical Research*, **92**, pp. 9693–9714.

Schertzer, D. and Lovejoy, S., 1991, *Nonlinear Variability in Geophysics: Scaling and Fractals* (Dordrecht: Kluwer Academic).

Schneising, O., Buchwitz, M., Burrows, J.P., Bovensmann, H., Bergamaschi, P. and Peters, W., 2009, Three years of greenhouse gas column-averaged dry air mole fractions retrieved from satellite – part 2 methane. *Atmospheric Chemistry and Physics*, **9**, pp. 443–445.

Schneising, O., Buchwitz, M., Burrows, J.P., Bovensmann, H., Reuter, M., Notholt, J., Macatangay, R. and Warneke, T., 2008, Three years of greenhouse gas column-averaged dry air mole fractions retrieved from satellite – part 1 carbon dioxide. *Atmospheric Chemistry and Physics*, **8**, pp. 3827–3853.

Sparling, L.C., 2000, Statistical perspectives on stratospheric transport. *Reviews of Geophysics*, **38**, pp. 417–436.

Sparling, L.C., Wei, J.C. and Avallone, L.M., 2006, Estimating the impact of small scale variability in satellite measurement validation. *Journal of Geophysical Research*, **111**, D20310, doi: 10.1029/2005JD006943.

Syroka, J. and Toumi, R., 2001, Scaling of Central England temperature fluctuations? *Atmospheric Science Letters*, **2**, pp. 143–154.

Toumi, R., Syroka, J., Barnes, C. and Lewis, P., 2001, Robust non-Gaussian statistics and long-range correlation of total ozone. *Atmospheric Science Letters*, **2**, pp. 94–103.

Tuck, A.F., 1989, Synoptic and chemical evolution of the Antarctic vortex in late winter and early spring 1987. *Journal of Geophysical Research*, **94**, pp. 11687–11737.

Tuck, A.F., 2008, *Atmospheric Turbulence: A Molecular Dynamics Perspective*, p. 33 (New York: Oxford University Press).

Tuck, A.F., 2010, From molecules to meteorology via turbulent scale invariance. *Quarterly Journal of the Royal Meteorological Society*, **136**, pp. 1125–1144.

Tuck, A.F. and Hovde, S.J., 1999, Fractal behavior of ozone, wind and temperature in the lower stratosphere. *Geophysical Research Letters*, **26**, pp. 1271–1274.

Tuck, A.F., Hovde, S.J. and Bui, T.P., 2004, Scale invariance in jet streams: ER-2 data around the lower stratospheric polar night vortex. *Quarterly Journal of the Royal Meteorological Society*, **130**, pp. 2423–2444.

Tuck, A.F., Hovde, S.J., Gao, R.-S. and Richard, E.C., 2003a, Law of mass action in the Arctic lower stratospheric polar vortex January–March 2000: ClO scaling and the calculation of ozone loss rates in a turbulent fractal medium. *Journal of Geophysical Research*, **108**, p. 4451.

Tuck, A.F., Hovde, S.J., Kelly, K.K., Mahoney, M.J., Proffitt, M.H., Richard, E.C. and Thompson, T.L., 2003b, Exchange between the upper tropical troposphere and the lower stratosphere studied with aircraft observations. *Journal of Geophysical Research*, **108**, p. 4734.

Tuck, A.F., Hovde, S.J. and Proffitt, M.H., 1999, Persistence in ozone scaling under the Hurst exponent as an indicator of the relative rates of chemistry and fluid mechanical mixing in the stratosphere. *Journal of Physical Chemistry A*, **103**, pp. 10445–10550.

Tuck, A.F., Hovde, S.J., Richard, E.C., Fahey, D.W. and Gao, R.-S., 2002, A scaling analysis of ER-2 data in the inner vortex during January–March 2000. *Journal of Geophysical Research*, **108**, p. 8306.

Tuck, A.F., Hovde, S.J., Richard, E.C., Gao, R.-S., Bui, T.P., Swartz, W.H. and Lloyd, S.A., 2005, Molecular velocity distributions and generalized scale invariance in the turbulent atmosphere. *Faraday Discussions*, **130**, pp. 181–193.

Varotsos, C., 2005, Power law correlations in column ozone over Antarctica. *International Journal of Remote Sensing*, **26**, pp. 3333–3342.

Varotsos, C. and Kirk-Davidoff, D., 2006, Long-memory processes in ozone and temperature variations at the region 60 degrees S – 60 degrees. *Atmospheric Chemistry and Physics*, **6**, pp. 4093–4100.

Yang, H. and Pierrehumbert, R., 1994, Production of dry air by isentropic mixing. *Journal of the Atmospheric Sciences*, **51**, pp. 3437–3451.